Using a global aerosol model adjoint to unravel the footprint of spatially-distributed emissions on cloud droplet number and cloud albedo

V.A. Karydis[1], S.L. Capps[2], R.H. Moore[3], A. Russell[4], D. K. Henze[5] and A. Nenes[1,2*]

[1] Earth and Atmospheric Sciences, Georgia Institute of Technology, Atlanta, GA

[2] Chemical and Biomolecular Engineering, Georgia Institute of Technology, Atlanta, GA

[3] NASA Langley Research Center, Hampton, VA

[4] Civil and Environmental Engineering, Georgia Institute of Technology, Atlanta, GA

[5] Department of Mechanical Engineering, University of Colorado, Boulder, CO

[*]Corresponding author: athanasios.nenes@gatech.edu

Abstract

The adjoints of the GEOS-Chem Chemical Transport Model and a comprehensive cloud droplet parameterization are coupled to study the sensitivity of cloud droplet number concentration (N_d) over US regions and Central Europe to global emissions of anthropogenic fine aerosol precursors. Simulations reveal that the N_d over the midwestern and southeastern US is mostly sensitive to SO_2 emissions during August, and to NH_3 emissions during February. Over the western US, N_d is mostly sensitivity to SO_2 and primary organic aerosol emissions. In Central Europe, N_d is most sensitive to NH_3 and NO_x emissions. As expected, local emissions strongly affect N_d; long-range transport, however, is also important for the western US and Europe. Emissions changes projected for the year 2050 are estimated to have the largest impacts on cloud albedo and N_d over Central Europe during August (42% and 82% change, respectively) and western US during February (12% and 36.5% change, respectively).

1. Introduction

Cloud droplets form upon pre-existing atmospheric aerosols, and their modulation from anthropogenic emissions has profound impacts on cloud radiative properties, the hydrological cycle and climate. The impact of aerosol on regional climate can be even stronger, owing to the variability of aerosol and regional climate sensitivity [*Shindell and Faluvegi*, 2009]. Attribution of climate forcing from sector-specific emissions is based on sequential perturbation calculations at the cost of a climate run per sector investigated [*Shindell et al.*, 2009]. This approach is frequently limited by addressing only one sector (e.g., transport [*Fuglestvedt et al.*, 2008]) or by invoking approximations required to reduce the computational burden (e.g., constant oxidant levels [*Koch et al.*, 2007]). Adjoint modeling provides an efficient sensitivity analysis alternative to brute-force approaches and does not require perturbations in emissions. This is accomplished by propagating a differential variation of a model output (e.g., aerosol concentration) backwards through the model to express its sensitivity with respect to inputs of interest (e.g., emissions) without perturbing the model state.

The GEOS-Chem chemical transport model (CTM) is a widely used global model for studying chemistry-aerosol-climate interactions [*Leibensperger et al.*, 2012a; b]. *Henze et al.* [2007] developed the adjoint of the code and since has been used e.g., to study black carbon over the Tibetan Plateau [*Kopacz et al.*, 2010]. Here the GEOS-Chem adjoint is coupled together with the adjoint of a comprehensive droplet parameterization [*Karydis et al.*, 2012] to quantify the influences of global emissions of primary organic aerosol (POA) and inorganic aerosol precursors (SO_2, NO_x, and NH_3) on the predicted cloud droplet number concentration (N_d) and cloud albedo (A) within three regions of the continental US and Central Europe during August and February for 2008 and 2050.

2. Model framework description

The GEOS-Chem model (v.9.1.1, http://geos-chem.org) is used to simulate the global aerosol distributions during February and August 2008, with 4^o by 5^o horizontal resolution and 47 pressure levels from the surface to 0.01 hPa. A detailed description of the model configuration and emissions is provided in the Supplementary Material. The adjoint of the GEOS-Chem model [*Henze et al.*, 2007] computes $\frac{\partial M_{a,tot}}{\partial E_{i,j}}$, the sensitivity of total aerosol mass concentrations, $M_{a,tot}$, to specific emissions E_i (where i is the emission type) for each grid cell j. In this study, $\frac{\partial M_{a,tot}}{\partial E_{i,j}}$ is calculated monthly for $M_{a,tot}$ on the final day of the month.

Calculation of N_d is carried out with the *Kumar et al.* [2009] parameterization; droplets are formed in ascending cloud parcels that contain soluble and insoluble particles competing for water vapor. The N_d adjoint [*Karydis et al.*, 2012] provides the sensitivity of N_d with respect to the parameterization input (updraft velocity, uptake coefficient and the number, hygroscopicity/adsorption parameters of each aerosol lognormal mode). The two adjoint frameworks elucidate the relationship of emissions to N_d by combining the local sensitivity of N_d to aerosol number concentration, $\left.\frac{\partial N_d}{\partial N_a}\right|_r$ (converted into local sensitivity of N_d to aerosol mass concentration, $\left.\frac{\partial N_d}{\partial M_a}\right|_r$, following the aerosol mass to number conversion as presented by Karydis et al. [2011]), with the sensitivity of total aerosol mass concentrations to anthropogenic emissions from each grid cell of the model, $\frac{\partial M_a}{\partial E_{i,j}}$, obtained from the GEOS-Chem adjoint. The result is the "footprint" (or impacts expressed as the sensitivity) of anthropogenic emissions from

each grid cell on the droplet number over the same region, $\frac{\partial N_{d,tot}}{\partial E_{i,j}} = \left(\sum_{r=1}^{R} \frac{\partial N_d}{\partial M_a}\bigg|_r \right)\left(\frac{\partial M_{a,tot}}{\partial E_{i,j}} \right)$, where R is the total number of cells in the region. The relative importance of anthropogenic emissions from each grid cell are presented as fully normalized sensitivities, $R_{i,j} = \frac{E_{i,j}}{N_d}\frac{\partial N_d}{\partial E_{i,j}} = \frac{\partial \ln N_d}{\partial \ln E_{i,j}}$, where $E_{i,j}$ is the emission of type i considered for grid cell j and N_d is the N_d over the region of study. $R_{tot,j}$ expresses the contribution of total anthropogenic emissions from grid cell j on N_d and $R_{i,tot}$ expresses the total (worldwide) contribution of anthropogenic emissions of type i (NH_3, SO_2, NO_x, or POA) on N_d. A detailed description of the sensitivity calculations is provided in the Supplementary Material.

The sensitivity results can be used to estimate the change in future N_d and cloud albedo, especially since adjoint sensitivities tend to be more robust than traditional source-receptor relationships determined from perturbing emissions across broad spatial scales [*Turner et al.*, [2012]. We consider projected aerosol precursor emissions following the Representative Concentration Pathway 4.5 (RCP4.5; supplementary material Table S2), where total radiative forcing is stabilized before 2100 by employment of a range of technologies and strategies for reducing greenhouse gas emissions [*Clarke et al.*, 2007]. Using the projected emissions change between 2010 and 2050, the change in N_d, ΔN_d, for each region is calculated for February and August. The first order change in cloud albedo (ΔA) is calculated from ΔN_d by integrating the susceptibility of A to N_d, $\frac{\partial A}{\partial N_d} = \frac{A(1-A)}{3N_d}$ [*Twomey*, 1991] over each region between 2010 and 2050 values. Cloud albedo at 2050, A_{2050}, is then given by $A_{2050} = \frac{C}{1+C}$, where

$C = \left(1 + \frac{\Delta N_d}{N_{d,2010}}\right)^{1/3} \left(\frac{A_{2010}}{1 - A_{2010}}\right)$ and A_{2010}, $N_{d,2010}$ are the local values of albedo and N_d at 2010, respectively. ΔA is then equal to A_{2050}-A_{2010}. Values of A_{2010} are obtained by differencing NASA CERES satellite total sky and clear sky albedos for February and August [*Acker and Leptoukh*, 2007] as described in *Moore et al.* [2012]. These calculations give an upper limit on albedo change since liquid water feedbacks which mitigate microphysical changes are not considered [*Stevens and Feingold*, 2009]. Given the lack of explicit microphysics in this study, a required assumption is that the aerosol number size distribution shape remains unchanged in the future. This may induce some error in the predicted sensitivity; as differences in aerosol microphysical processes may change the relationship between emissions and CCN concentrations. Toward this, Manktelow et al. [2009] found that the aerosol number potential of N. American and Asian emissions was a factor of 3 to 4 times larger than that of European emissions, resulting in a 70% more efficient production of CCN.

3. Results and Discussion

Figure 1 presents the fully normalized sensitivity of regional N_d to anthropogenic emissions from each grid cell. Figure 2a and 2b depict the total worldwide contribution of anthropogenic emissions on N_d as well as the fractional contribution of these anthropogenic emissions from within each region for present and future (based on RCP4.5 scenario) conditions, respectively. An analysis of each region and species follows.

Midwestern US: N_d is mostly sensitive to SO_2 ($R_{SO2,tot} = 8.6\times10^{-2}$) and NO_x ($R_{NOx,tot} = 3.4\times10^{-2}$) during August, and to NH_3 emissions during February ($R_{NH3,tot} = 6.3\times10^{-2}$). Moreover, the high impact of NH_3 emissions on N_d during February together with the low impact of NO_x emissions, confirms that NH_3 is the limiting reactant in the formation of ammonium nitrate during the

winter in this area. POA emissions have relatively low impact (~0.5×10^{-2}) on N_d, (Figure 2) owing to the lower magnitude of the primary organic emissions, compared to inorganic precursors over the midwestern US. The importance of NH_3 emissions in February and SO_2 emissions in August to aerosol formation over the midwestern US was also confirmed by *Tsimpidi et al.* [2007]. *Henze et al.* [2009] also predicted similar trends for the sensitivity of inorganic aerosols to NH_3 and SO_2, however, the predicted effect on N_d is less pronounced as only a small fraction of aerosols is activated into droplets (<5%) over the polluted continental environments such as midwestern US. The lower impact of NO_x emissions on N_d during February is in accordance with *Tsimpidi et al*. [2008], who attributed this behavior to the increase of oxidants levels (after a NO_x emission reduction during winter) which promoted secondary aerosol production and compensated for the decrease of nitrates. In August, sulfate is the dominant inorganic aerosol component; therefore, aerosol concentrations are more sensitive to SO_2 emission changes from electricity generating units, followed by NO_x emissions, while NH_3 emissions have little impact (Figure 2). N_d is predicted to decrease by 75.62 cm^{-3} (9.87%) and 26.05 cm^{-3} (3.4%) due to SO_2 and NO_x emission changes by 2050, respectively (Table S3). During February, SO_2 emission decreases will increase the free NH_3 in the atmosphere, resulting in an increase in ammonium nitrate concentration. Therefore, sulfate is replaced by nitrate in the aerosol phase resulting in a minimal negative response of N_d to SO_2 emission changes ($R_{SO2,tot}$ = -0.28×10^{-2}). The negative sensitivity arises from sufficiently low temperatures and high concentrations of HNO_3 at which the addition of one mole of SO_4^{-2} to the aerosol can actually reduce the total mass by displacing two moles of NO_3^- [*Moya et al.*, 2002; *West et al.*, 1999]. Overall, during August, N_d and A are predicted to decrease in 2050 by ~100 cm^{-3} (13.2% change from 2010 levels) and ~4×10^{-3} (4.2%), respectively (supplementary material, Table S3). During

February, ΔA and ΔN_d are predicted to be very low (Table S3). In this case, $R_{SO2,tot}$ and $R_{NOx,tot}$ are very small, while $R_{NH3,tot}$ is high (and NH_3 emissions are expected to slightly increase in the future) (Figure 2a) so emissions changes have a small impact on N_d and A.

Southeastern US: N_d over the southeastern US is more sensitive to SO_2 electricity generation emissions during both seasons (5.9×10^{-2}) followed by NH_3 emissions from agriculture during February (5.1×10^{-2}) and NO_x emissions from electricity generating units during August (2.8×10^{-2}) (Figure 2). Consistent with *Capps et al.* [2012], the low amounts of nitric acid and ammonia not "bound" to sulfate leads to low levels of aerosol ammonium nitrate. This means that the aerosol cannot buffer SO_2 emissions shifts. N_d is predicted to decrease by 39 cm^{-3} (5.9%) and 57 cm^{-3} (10%) due to SO_2 emission changes by 2050 during August and February, respectively, and by 16 cm^{-3} (2.5%) due to NO_x emissions changes during August (Table S3). Anthropogenic POA emissions have an important impact during both February and August ($R_{NH3,tot}$ =2.2×10^{-2} and 1.1×10^{-2}, respectively). Nevertheless, the predicted N_d change attributed to POA emission changes by 2050 is negligible (less than 0.1%) since the latter is not expected to change significantly over US (Table S2). Overall, N_d and A are predicted to decrease in 2050 by ~53.3 cm^{-3} (8.3%) and 3.5×10^{-3} (2.5%), respectively, during August and by 56.7 cm^{-3} (10%) and 5.1×10^{-3} (2.8%), respectively, during February (Table S3).

Western US: Anthropogenic SO_2 emissions are found to be the most important contributor to cloud droplet formation over the western US during both February and August ($R_{SO2,tot}$ = 12.8×10^{-2} and 6×10^{-2}, respectively) (Figure 2). SO_2 emissions contribution to N_d over western US is similar (during August) or even higher (during February) than the corresponding contribution to N_d over midwestern and southeastern US, despite the fact that typically SO_2 emissions are lower in western US. This can be explained by the high sensitivity of N_d to SO_2

153 from long range transport, especially from eastern China, resulting in a significant decrease of N_d
154 in 2050 (52.6 cm^{-3} or 20.5%) due to changes on SO_2 emissions outside the western US. SO_2
155 emissions from shipping also contribute significantly to N_d. POA anthropogenic emissions also
156 significantly impact the N_d over the West, especially during February ($R_{POA,tot}$ = 6.7×10^{-2}).
157 Similarly to southeastern US though, the predicted ΔN_d in 2050 due to POA emission changes is
158 low (Table S3). Anthropogenic NH_3 emissions during August and anthropogenic NO_x emissions
159 during February do not impact N_d over the West ($R_{NOx,tot}$ = 0.5×10^{-2} and 1.7×10^{-2}, respectively)
160 (Figure 2). Although highly concentrated centers of agricultural or urban activity emit significant
161 amounts of NO_x and NH_3, respectively, pristine surrounding land causes dilution that limits the
162 apparent impact on aerosol formation. Overall, N_d and A are predicted to decrease in 2050 by
163 ~52.6 cm^{-3} (12.2%) and 2.6×10^{-3} (4%), respectively, during August and by 93.5 cm^{-3} (36.5%)
164 and 17.1×10^{-3} (12.3%), respectively, during February (Table S3). The strong effect of long-range
165 transport of pollutants is mostly evident during February where the 57% of the predicted ΔN_d in
166 2050 is attributed to changes on anthropogenic emissions from outside the western US.
167 *Central Europe:* N_d is mostly sensitive to NH_3 ($R_{NH3,tot}$ = 11.7×10^{-2}) and NO_x ($R_{NOx,tot}$ = 10.6×10^{-2})
168 emissions during both August and February ($R_{NH3,tot}$ = 5.7×10^{-2} and $R_{NOx,tot}$ = 7.1×10^{-2}). POA
169 emissions impact N_d negligibly over Central Europe during both seasons ($R_{POA,tot}$ as low as
170 0.2×10^{-2}). These conclusions are consistent with *Megaritis et al.* [2012] who found that NH_3
171 emissions had the most significant impact on aerosol formation over Europe, while the impact of
172 POA emissions was the smallest. Ammonium nitrate is a major aerosol component over Europe;
173 therefore, emissions of its gas phase precursors (NH_3 and NO_x) exhibit the strongest impact on
174 the inorganic aerosol population and N_d. However, according to RCP4.5 scenario, emissions of
175 NH_3 over central Europe are not expected to change significantly by 2050 (0.06% increase). On

the other hand, changes on NO_x emissions result to significant changes on ΔN_d (315 cm^{-3} or 50% and 74 cm^{-3} or 10% during August and February , respectively). SO_2 also contributes with a similar magnitude to N_d over central Europe during August ($R_{SO2,tot} = 6.7\times10^{-2}$). N_d is predicted to decrease by 230 cm^{-3} (37%) due to SO_2 emission changes by 2050 and is strongly influenced by long-range transport of SO_2 from Midwestern and northeastern US. The predicted ΔN_d due to changes of anthropogenic SO_2 emissions from outside the central Europe during August is 230 cm^{-3} (23%). During February, when sulfate levels are lower, N_d is less sensitive to SO_2 emissions ($R_{SO2,tot} = 0.8\times10^{-2}$), likely due to the limited H_2O_2 availability over Europe during this season [*Megaritis et al.*, 2012]. Overall, ΔN_d decrease by 510 cm^{-3} (82%) and ΔA by 31.86 $\times10^{-3}$ (42%,) during August. The large $R_{SO2,tot}$ and $R_{NOx,tot}$ predicted over Europe during this season (Figure 2), together with the large future reductions of these emissions (e.g., SO_2; Figure 1) results in the strong response of N_d and A to future emission changes, which is also influenced by the long-range impact of SO_2 emission reductions from the US (Figure 1). During February, ΔN_d and ΔA are predicted to be 77 cm^{-3} (10.7%) and 4.2 $\times10^{-3}$ (3.2%,), respectively, and are mostly attributed to NO_x emissions (Table S3).

4. Conclusions

In this work, the adjoints of the GEOS-Chem CTM and Kumar et. al [2009] droplet parameterization are used to determine the source region and relative impact of aerosol precursor emissions on N_d and albedo. Assessments are carried out for specific regions in February and August of 2008 and 2050 (using the RCP4.5 scenario). Among all species, the influence of sulfate emissions in August is most similar across regions, comprising at least 50% (20%) of the total influence in the US regions (Central Europe). For each region, the percent contribution

from sulfate emissions within the region is the lowest of all the species tracked, which implicates long-range transport of significant sulfate burdens. Central Europe N_d in August is far more influenced by NH_3 and NO_x emissions than any region over the US due to the large contribution of ammonium nitrate aerosol to the regional aerosol. Nevertheless, for all four regions, 65-85% of the influence from NH_3 and NO_x emissions came from within the region in August. In February, the influence of NO_x emissions on Central Europe N_d remains much higher than on the N_d over US regions. However, the impact of NH_3 emissions on N_d, during February, is similar for Central Europe, midwestern, and southeastern US. Additionally, the maximum percent contribution of NO_x emissions within the region (nearly 100%) is attained in the western and southeastern US in February. The strongest internal influence is from POA in both August and February, owing to the shorter lifetime of the species. With the exception of the western US, the relative influence of POA on N_d is minor. The influence of different emissions mixes on N_d is most apparent from the distinction between the US and European response to NO_x and NH_3 emissions. Based on the RCP4.5 scenario and the 2008 adjoint, A in Central Europe during August and in western US during February is most strongly affected by future emission changes, owing to the effects of long-range transport of anthropogenic emissions (mainly SO_2) and NO_x reductions over Central Europe and the western US. The significant decrease of N_d over these regions results in higher anthropogenic emissions contributions to N_d in 2050 as the maximum supersaturation and droplet activation fractions are increased [Karydis et al., 2012]. In other regions and seasons, the anthropogenic emissions contributions to N_d are lower in 2050, mainly due to the significant decrease of SO_2 and NO_x emissions over the US and Europe (figure 2b). The above results reveal N_d sensitivities that would not have been predicted from earlier forward sensitivity analyses, i.e. the importance of SO_2 long-range transport on N_d over western US or the

increasing contribution of SO_2 to N_d over central Europe in the future, and can be used from policy makers to effectively design future emission control strategies.

Understanding relative impacts in coupled complex models is a challenge. Using the coupled adjoint sensitivity modeling framework developed here has allowed us to quantify the sensitivity of cloud droplet formation and cloud albedo to different aerosol precursor emissions and to unravel the importance of sectoral, spatial, and seasonal emissions.

Acknowledgments

We acknowledge support from NASA-ACMAP and NOAA. SLC gratefully acknowledges the NSF GRF and NASA ESSF. DKH Acknowledges support from a NASA New Investigator grant.We also thank two anonymous reviewers for comments that improved the manuscript.

References

Acker, J. G., and G. Leptoukh (2007), Online analysis enhances use of NASA Earth science data, *Eos Transactions*, *88*(14).

Bauer, S. E., Y. Balkanski, M. Schulz, D. A. Hauglustaine, and F. Dentener (2004), Global modeling of heterogeneous chemistry on mineral aerosol surfaces: Influence on tropospheric ozone chemistry and comparison to observations, *J. Geophys. Res.-Atmos.*, *109*(D2).

Bouwman, A. F., D. S. Lee, W. A. H. Asman, F. J. Dentener, K. W. VanderHoek, and J. G. J. Olivier (1997), A global high-resolution emission inventory for ammonia, *Glob. Biogeochem. Cycle*, *11*(4), 561-587.

Clarke, L., J. Edmonds, H. Jacoby, H. Pitcher, J. Reilly, and R. Richels (2007), Scenarios of Greenhouse Gas Emissions and Atmospheric Concentrations.*Rep. 2.1A of Synthesis and Assessment Product 2.1 by the U.S. Climate Change Science Program and the Subcommittee on Global Change Research*, 154 pp, Department of Energy, Office of Biological & Environmental Research, Washington, DC., USA.

Fountoukis, C., and A. Nenes (2007), ISORROPIA II: a computationally efficient thermodynamic equilibrium model for K+-Ca2+-Mg2+-Nh(4)(+)-Na+-SO42--NO3--Cl--H2O aerosols, *Atmospheric Chemistry and Physics*, *7*(17), 4639-4659.

Fuglestvedt, J., T. Berntsen, G. Myhre, K. Rypdal, and R. B. Skeie (2008), Climate forcing from the transport sectors, *Proceedings of the National Academy of Sciences of the United States of America*, *105*(2), 454-458.

Guenther, A., T. Karl, P. Harley, C. Wiedinmyer, P. I. Palmer, and C. Geron (2006), Estimates of global terrestrial isoprene emissions using MEGAN (Model of Emissions of Gases and Aerosols from Nature), *Atmospheric Chemistry and Physics*, *6*, 3181-3210.

Henze, D. K., A. Hakami, and J. H. Seinfeld (2007), Development of the adjoint of GEOS-Chem, *Atmos. Chem. Phys.*, *7*(9), 2413-2433.

Henze, D. K., J. H. Seinfeld, and D. T. Shindell (2009), Inverse modeling and mapping US air quality influences of inorganic PM2.5 precursor emissions using the adjoint of GEOS-Chem, *Atmospheric Chemistry and Physics*, *9*(16), 5877-5903.

Jacobson, M. Z. (1999), Studying the effects of calcium and magnesium on size-distributed nitrate and ammonium with EQUISOLV II, *Atmospheric Environment*, *33*(22), 3635-3649.

Jaffe, D., I. McKendry, T. Anderson, and H. Price (2003), Six 'new' episodes of trans-Pacific transport of air pollutants, *Atmos. Environ.*, *37*(3), 391-404.

Karydis, V. A., S. L. Capps, A. G. Russell, and A. Nenes (2012), Adjoint sensitivity of global cloud droplet number to aerosol and dynamical parameters, *Atmos. Chem. Phys. Discuss.*, *12*(5), 12081-12117.

Karydis, V. A., P. Kumar, D. Barahona, I. N. Sokolik, and A. Nenes (2011), On the effect of dust particles on global cloud condensation nuclei and cloud droplet number, *J. Geophys. Res.-Atmos.*, *116*.

Koch, D., T. C. Bond, D. Streets, and N. Unger (2007), Linking future aerosol radiative forcing to shifts in source activities, *Geophys. Res. Let.*, *34*(L05821).

Kopacz, M., et al. (2010), Global estimates of CO sources with high resolution by adjoint inversion of multiple satellite datasets (MOPITT, AIRS, SCIAMACHY, TES), *Atmospheric Chemistry and Physics*, *10*(3), 855-876.

Kuhns, H., E. M. Knipping, and J. M. Vukovich (2005), Development of a United States-Mexico emissions inventory for the Big Bend Regional Aerosol and Visibility Observational (BRAVO) Study, *Journal of the Air & Waste Management Association*, *55*(5), 677-692.

Kumar, P., I. N. Sokolik, and A. Nenes (2009), Parameterization of cloud droplet formation for global and regional models: including adsorption activation from insoluble CCN, *Atmos. Chem. Phys.*, *9*(7), 2517-2532.

Leibensperger, E. M., L. J. Mickley, D. J. Jacob, W. T. Chen, J. H. Seinfeld, A. Nenes, P. J. Adams, D. G. Streets, N. Kumar, and D. Rind (2012a), Climatic effects of 1950-2050 changes in US anthropogenic aerosols - Part 1: Aerosol trends and radiative forcing, *Atmos. Chem. Phys.*, *12*(7), 3333-3348.

Leibensperger, E. M., L. J. Mickley, D. J. Jacob, W. T. Chen, J. H. Seinfeld, A. Nenes, P. J. Adams, D. G. Streets, N. Kumar, and D. Rind (2012b), Climatic effects of 1950-2050 changes in US anthropogenic aerosols - Part 2: Climate response, *Atmos. Chem. Phys.*, *12*(7), 3349-3362.

Manktelow, P. T., K. S. Carslaw, G. W. Mann, and D. V. Spracklen (2009), Variable CCN formation potential of regional sulfur emissions, *Atmospheric Chemistry and Physics*, *9*(10), 3253-3259.

Megaritis, A. G., C. Fountoukis, P. E. Charalampidis, C. Pilinis, and S. N. Pandis (2012), Response of fine particulate matter concentrations to changes of emissions and temperature in Europe, *Atmos. Chem. Phys. Discuss.*, *12*(4), 8771-8822.

Moore, R. H., V. A. Karydis, S. L. Capps, T. L. Lathem, and A. Nenes (2012), Droplet Number Prediction Uncertainties From CCN: An Integrated Assessment Using Observations and a Global Adjoint Model, *Atmos. Chem. Phys. Discuss.* , *submitted*.

Moya, M., S. N. Pandis, and M. Z. Jacobson (2002), Is the size distribution of urban aerosols determined by thermodynamic equilibrium? An application to Southern California, *Atmospheric Environment*, *36*(14), 2349-2365.

Olivier, J. G. J., and J. J. M. Berdowski (2001), Global emissions sources and sinks, in *The Climate System*, edited by J. Berdowski, Guicherit, R. and B.J. Heij, pp. 33-78, A.A. Balkema Publishers/Swets & Zeitlinger Publishers, Lisse, The Netherlands.

Shindell, D. T., G. Faluvegi, D. M. Koch, G. A. Schmidt, N. Unger, and S. E. Bauer (2009), Improved Attribution of Climate Forcing to Emissions, *Science*, *326*(5953), 716-718.

Stevens, B., and G. Feingold (2009), Untangling aerosol effects on clouds and precipitation in a buffered system, *Nature*, *461*(7264), 607-613.

Streets, D. G., et al. (2003), An inventory of gaseous and primary aerosol emissions in Asia in the year 2000, *J. Geophys. Res.-Atmos.*, *108*(D21).

Tsimpidi, A. P., V. A. Karydis, and S. N. Pandis (2007), Response of inorganic fine particulate matter to emission changes of sulfur dioxide and ammonia: The eastern United States as a case study, *J. Air Waste Manage. Assoc.*, *57*(12), 1489-1498.

Tsimpidi, A. P., V. A. Karydis, and S. N. Pandis (2008), Response of Fine Particulate Matter to Emission Changes of Oxides of Nitrogen and-Anthropogenic Volatile Organic Compounds in the Eastern United States, *J. Air Waste Manage. Assoc.*, *58*(11), 1463-1473.

Turner, A. J., D. K. Henze, R. V. Martin, and A. Hakami (2012), The spatial extent of source influences on modeled column concentrations of short-lived species, *Geophys. Res. Lett.*, *39*(12), L12806.

Twomey, S. (1991), Aerosols, clouds and radiation, *Atmos. Environ. Part a-General Topics*, *25*(11), 2435-2442.

van der Werf, G. R., J. T. Randerson, L. Giglio, G. J. Collatz, P. S. Kasibhatla, and A. F. Arellano, Jr. (2006), Interannual variability in global biomass burning emissions from 1997 to 2004, *Atmospheric Chemistry and Physics*, *6*, 3423-3441.

West, J. J., A. S. Ansari, and S. N. Pandis (1999), Marginal PM2.5: Nonlinear aerosol mass response to sulfate reductions in the Eastern United States, *J. Air Waste Manage. Assoc.*, *49*(12), 1415-1424.

Wolff, G. T. (1984), On the nature of nitrate in coarse continental aerosols, *Atmospheric Environment*, *18*(5), 977-981.

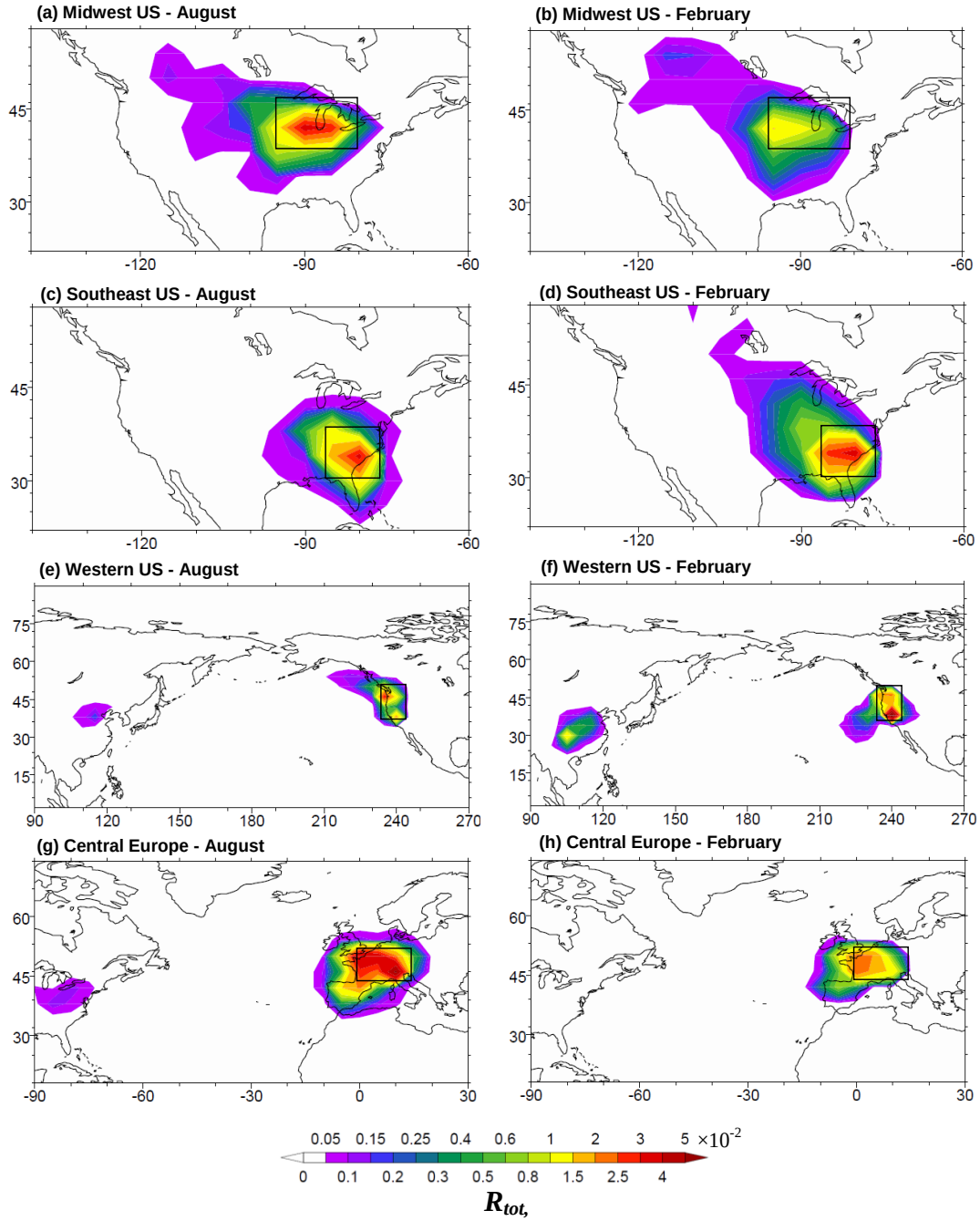

Figure 1: Contribution of total anthropogenic emissions to cloud droplet number concentration over Midwest US (a, b), Southeast US (c, d), Western US (e, f), and Central Europe (g, h) during August (left column) and February (right column) of 2008. The regions of study are denoted by the squares.

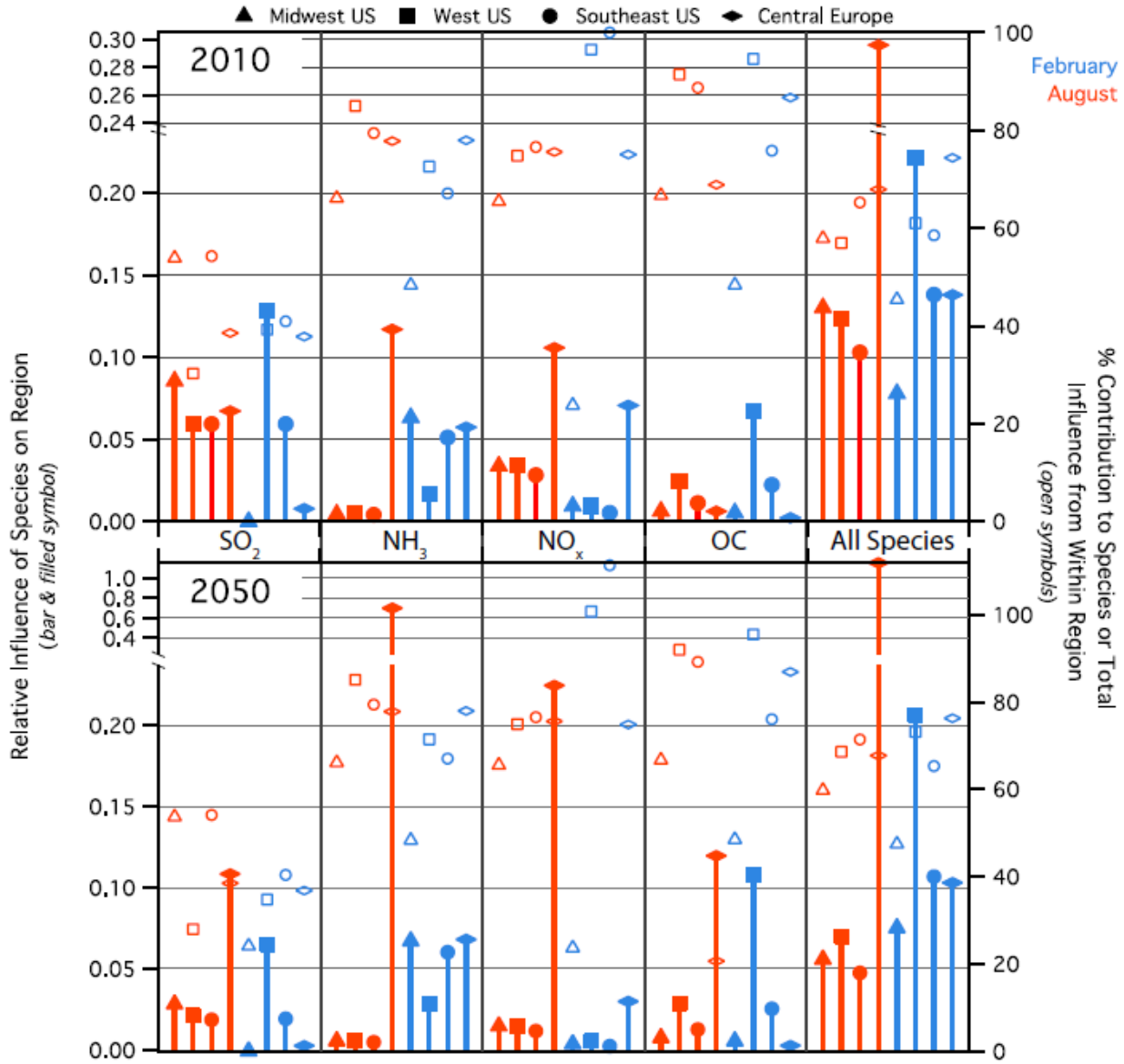

Figure 2: Total contribution of anthropogenic SO_2, NO_x, NH_3, and OC emissions to N_d over Midwest US, Southeast US, Western US, and Central Europe during August (orange) and February (blue) of 2010 (top panel) and 2050 (bottom panel). The fractional contribution of anthropogenic emissions from within each region on N_d is also shown (open symbols).

Supplementary Material

1. Model framework description

The GEOS-Chem model is driven using assimilated meteorological data from the Goddard Earth Observing System (GEOS-5) of the NASA Global Modeling and Assimilation Office (GMAO) [*Fountoukis and Nenes*, 2007] and includes gas-phase chemistry coupled with heterogeneous reactions, inorganic aerosol thermodynamics, and oxidative aging of carbonaceous aerosols [*Bauer et al.*, 2004]. NH_3 emissions are from the Global Emission Inventory Activity (GEIA) inventory [*Bouwman et al.*, 1997]. Biogenic VOCs follow the Model of Emissions of Gases and Aerosols from Nature (MEGAN) inventory [*Guenther et al.*, 2006]. NO_x and SO_x emissions are obtained from the Emissions Database for Global Atmospheric Research (EDGAR) inventory [*Olivier and Berdowski*, 2001]]. These global inventories are overwritten with regional inventories for the US (NEI99), Europe (EMEP), southeast Asia [*Streets et al.*, 2003], and Mexico (BRAVO) [*Kuhns et al.*, 2005]. Biomass burning emissions are from *van der Werf et al.* [2006].

Aerosol mass concentrations from GEOS-Chem follow a prescribed number size distribution (Table S1) according to *Karydis et al.* [2012] and distributed in three externally mixed modes: *i*) sulfate, ammonium, nitrate, organics, and black carbon from anthropogenic and biomass burning sources, *ii*) sulfate, nitrate, and sea salt from marine processes, and, *iii*) mineral dust. Sensitivity to secondary organic aerosol (SOA) is not considered, as GEOS-Chem does not produce adjoint sensitivities of SOA mass to volatile organic carbon emissions. Following Karydis et al. [2011], the number concentration of each aerosol mode is given by $N_a = \frac{m_{tot}}{V \rho_{tot}}$ where m_{tot} is the total mass concentration of the aerosol mode, V is the volume of the dry aerosol, and ρ_{tot} is the density of the aerosol given by $\rho_{tot} = \frac{m_{tot}}{\sum_{y=1}^{Y} \frac{m_y}{\rho_y}}$. m_y is the mass

concentration of each component within the aerosol mode (e.g. sulfate, nitrate, ammonium, OC, BC), ρ_y is its density and Y is the number of aerosol components. The hygroscopicity of each aerosol mode is calculated based on the aerosol composition, provided by GEOS-Chem, and is given by $\kappa = \frac{VH_{f,tot}\rho_{tot}V_{f,s}M_w}{M_s\rho_w}$, where $V_{f,s}$ is the soluble volume fraction, M_w and M_s is the molecular weight of water and soluble fraction respectively, ρ_w is the density of water, and, $VH_{f,tot}$ is the total Van't Hoff factor of soluble fraction given by $VH_{f,tot} = \frac{\sum_{y=1}^{YS}\frac{m_y VH_{f,y}}{M_y}}{\sum_{y=1}^{YS}\frac{m_y}{M_y}}$, where *YS* is the number of aerosol soluble components ,$VH_{f,y}$ is the Van't Hoff factor of each soluble aerosol component and M_y is the molecular weight of each soluble aerosol component. Other important parameters for N_d calculations are presented by *Karydis et al.* [2012].

2. Computing sensitivities of N_d to anthropogenic aerosol emissions and ΔN_d due to future anthropogenic emissions changes

Figure 1 of the main text presents the fully normalized sensitivity (unitless) of regional N_d to anthropogenic emissions from each grid cell:

$$R_{i,j} = \sum_{r=1}^{R}\left(\left(\frac{N_{a,r}}{N_{d,r}}\frac{\partial N_{d,r}}{\partial N_{a,r}}\right)\sum_{y=1}^{Y}\left(\frac{M_{a,r,y}}{N_{a,r}}\frac{\partial N_{a,r}}{\partial M_{a,r,y}}\right)\right)\left(\frac{E_{i,j}}{\sum_{r,y=[1,1]}^{[R,Y]}M_{a,r,y}}\frac{\partial\sum_{r,y=[1,1]}^{[R,Y]}M_{a,r,y}}{\partial E_{i,j}}\right) = \frac{E_{i,j}}{\sum_{r=1}^{R}N_{d,r}}\frac{\partial\sum_{r=1}^{R}N_{d,r}}{\partial E_{i,j}} = \frac{\partial \ln N_d}{\partial \ln E_{i,j}},$$

where $E_{i,j}$ is the emission of type i considered for grid cell j, $N_{d,r}$ and $N_{a,r}$ are the are the aerosol number and droplet number concentrations for regional grid cell r, respectively, $M_{a,r,y}$ is the aerosol mass concentration of species y for regional grid cell r, and N_d is the total droplet number concentration over the region of study. The first term,

$\sum_{r=1}^{R}\left(\left(\frac{N_{a,r}}{N_{d,r}}\frac{\partial N_{d,r}}{\partial N_{a,r}}\right)\sum_{y=1}^{Y}\left(\frac{M_{a,r,y}}{N_{a,r}}\frac{\partial N_{a,r}}{\partial M_{a,r,y}}\right)\right)$, is the fully normalized adjoint sensitivity of total droplet number to aerosol mass concentration, over the region of study, from the droplet activation parameterization; the second term, $\left(\frac{E_{i,j}}{\sum_{r,y=[1,1]}^{[R,Y]} M_{a,r,y}}\frac{\partial \sum_{r,y=[1,1]}^{[R,Y]} M_{a,r,y}}{\partial E_{i,j}}\right)$, is the fully normalized adjoint sensitivity of aerosol mass concentration, over the region of study, to anthropogenic emissions of type i considered for grid cell j, calculated by GEOS-Chem adjoint. The above sensitivity calculations are made only for the aerosol mode containing sulfate, ammonium, nitrate, organics, and black carbon, since currently GEOS-Chem does not produce adjoint sensitivities to sea salt and dust emissions.

Figure 2a of the main text depicts the total worldwide contribution of anthropogenic emissions to present N_d (unitless): $R_{i,tot} = \sum_{j=1,n}\frac{\partial \ln N_d}{\partial \ln E_{i,j}}$, where i is the emission type and n is the total number of grid cells.

Figure 2b of the main text depicts the total worldwide contribution of anthropogenic emissions to future N_d (unitless): $R_{i,tot} = \sum_{j=1,n}\left(\frac{\partial \ln N_d}{\partial \ln E_{i,j}}\frac{\left(1+\Delta E_{i,j}\right)}{\left(1+\Delta N_d\right)}\right)$, where $\Delta E_{i,j}$ and ΔN_d are the fractional change of emissions $\left(\frac{E_{i,j,2050}-E_{i,j,2010}}{E_{i,j,2010}}\right)$ and droplet number $\left(\frac{N_{d,2050}-N_{d,2010}}{N_{d,2010}}\right)$ from Table S2 and Table S3, respectively.

Table S3 presents the change in N_d (cm^{-3}) due to future emissions changes: $\left(\frac{\partial N_d}{\partial M_a}\right)\left(E_{i,j}\frac{\partial M_a}{\partial E_{i,j}}\right)\Delta E_{i,j} = \frac{\partial N_d}{\partial E_{i,j}}\left(E_{i,j,2050} - E_{i,j,2010}\right)$. The first term, $\left(\frac{\partial N_d}{\partial M_a}\right)$, is the un-normalized adjoint sensitivity of droplet number to aerosol mass concentration, over the region of study, from the droplet activation parameterization, while the second term, $\left(E_{i,j}\frac{\partial M_a}{\partial E_{i,j}}\right)$, is the semi-normalized adjoint sensitivity of aerosol mass concentration, over the region of study, to anthropogenic emissions of type *i* considered for grid cell *j*, calculated by GEOS-Chem adjoint. The third term, $\Delta E_{i,j}$, is the fractional change of emissions from Table S2.

3. R_{ij} and emissions contributions to N_d for each region

Midwestern US: During August, emissions from within the Midwest contribute ~60% of the N_d, with values of $R_{tot,j}$ up to 3.4×10^{-2} over Illinois (Figure 1a of main text). Emissions from South and Southwest Canada notably contribute to N_d (up to 0.15×10^{-2}). During February, the predicted impact of anthropogenic emissions on N_d over the Midwest US covers a larger region, with the impact of emissions from Canada being more important.

Southeastern US: Emissions from within the region have the largest impact (60-65%) on N_d in the region ($R_{tot,j}$ up to 3.4×10^{-2}) during both February and August (Figure 1c,1d, and 2 of main text). Emissions from the Midwest also impact regional N_d during both seasons ($R_{tot,j}$ up to 1×10^{-2}). This impact is mostly due to SO_2 emissions during summer and NH_3 emissions during winter. N_d is affected by emissions (mainly NH_3) from south-central Canada during February ($R_{NH3,tot}$ up to 0.1×10^{-2}).

Western US: N_d is strongly affected by regional emissions (over California during February, $R_{tot,j}$ = 6.5×10^{-2}, and over Washington state during August, $R_{tot,j}$ = 2.9×10^{-2}; Figure 1e, 1f of main text). Long-range transport of anthropogenic emissions from Asia [e.g., *Jaffe et al.*, 2003; *Wolff*, 1984] also impacts significantly cloud droplet formation over the western US, especially during February ($R_{tot,j}$ up to 1.5×10^{-2} for Eastern China) and accounts approximately for one third of the total sensitivity of emission impacts on N_d over the western US.

Central Europe: During August, anthropogenic emissions from northern Italy (Po Valley), have the largest impact on N_d over Central Europe ($R_{tot,j}$ up to 5.3×10^{-2}, Figure 1g of main text). Anthropogenic emissions from the northeastern and midwestern US also contribute about 4% to the N_d over Europe ($R_{tot,j}$ up to 0.2×10^{-2}). Due to the prevalent winds during February, N_d is more sensitive to anthropogenic emissions over France with $R_{tot,j}$ up to 2.4×10^{-2} (Figure 1h of main text).

Table S1. Size distribution parameters applied to aerosol populations from GEOS-Chem model

Aerosol type	Aerosol components	Density (g cm^{-3})	Median diameter (μm)	Geometric standard deviation	Number fraction	Reference
Anthropogenic, Biomass Burning	Sulfate	1.77	0.1	1.9	1	Chuang et al. [1997]; Radke et al. (1988)
	Nitrate	1.725				
	Ammonium	1.75				
	Organic Carbon	1.2				
	Black Carbon	1.5				
Marine	Sulfate	1.77	0.018	1.4	0.81	Lance et al. [2004]
	Nitrate	1.725	0.075	1.6	0.18	
	Sea Salt	2.2	0.62	2.7	0.01	
Mineral Dust	Mineral Dust	2.6	0.16	2.1	0.93	D'Almeida et al. [1987]
			1.4	1.9	0.07	
			10	1.6	3×10^{-6}	

Table S2: Fractional emission change (2010-2050) for SO_2, NH_3, NO_x, and primary OC based on RCP4.5 scenario. Negative values correspond to a decrease from 2010 to 2050.

Region	SO_2	NH_3	NO_x	Primary OC
Western Europe, Northern America, Australia, Japan	-0.72	0.06	-0.62	0.02
Eastern Europe, Russia	-0.69	0.03	-0.50	-0.10
Asia	-0.64	0.12	-0.24	-0.52
Middle East, Africa	-0.05	0.20	0.04	0.00
Latin and Central America	-0.49	0.06	-0.23	-0.42

Table S3: Change (2010-2050) in droplet number (cm^{-3}) and shortwave cloud albedo from emissions changes based on RCP4.5 scenario. Negative values correspond to a decrease from 2010 to 2050. Numbers in parentheses represent the percentile change (%) of droplet number and cloud albedo.

Region	ΔN_d from SO_2	ΔN_d from NH_3	ΔN_d from NO_x	ΔN_d from primary OC	Total ΔN_d	ΔA from Total ΔN_d ($\times 10^{-3}$)
Midwestern US August	-75.62 (-9.87)	0.34 (0.04)	-26.05 (-3.4)	0.18 (0.03)	-101.15 (-13.2)	4.08 (4.2)
Midwestern US February	2.47 (0.42)	4.64 (0.77)	-7.13 (-1.18)	0.15 (0.02)	0.12 (0.02)	-0.001 (-0.005)
Southeastern US August	-39.02 (-5.92)	0.22 (0.04)	-15.78 (-2.45)	0.24 (0.08)	-53.34 (-8.3)	3.47 (2.5)
Southeastern US February	-57.24 (-9.99)	4.22 (0.74)	-4.37 (-0.77)	0.67 (0.12)	-56.71 (-9.9)	5.12 (2.8)
Western US August	-35.03 (-8.12)	0.24 (0.06)	-18.17 (-4.22)	0.36 (0.09)	-52.59 (-12.2)	2.58 (4.0)
Western US February	-89.64 (-34.99)	1.28 (0.5)	-6.25 (-2.44)	1.08 (0.43)	-93.53 (-36.5)	17.13 (12.3)
Central Europe August	-229.29 (-37)	33.55 (5.42)	-314.99 (50.83)	0.70 (0.11)	-510.03 (-82.3)	31.86 (41.9)
Central Europe February	-9.16 (-1.28)	5.75 (0.8)	-73.54 (-10.24)	0.09 (0.01)	-76.86 (-10.7)	4.21 (3.2)

References

Bauer, S. E., Y. Balkanski, M. Schulz, D. A. Hauglustaine, and F. Dentener (2004), Global modeling of heterogeneous chemistry on mineral aerosol surfaces: Influence on tropospheric ozone chemistry and comparison to observations, *J. Geophys. Res.-Atmos.*, *109*(D2).

Bouwman, A. F., D. S. Lee, W. A. H. Asman, F. J. Dentener, K. W. VanderHoek, and J. G. J. Olivier (1997), A global high-resolution emission inventory for ammonia, *Glob. Biogeochem. Cycle*, *11*(4), 561-587.

Chuang, C. C., J. E. Penner, K. E. Taylor, A. S. Grossman, and J. J. Walton (1997), An assessment of the radiative effects of anthropogenic sulfate, *J. Geophys. Res.*, *102*(D3), 3761-3778.

D'Almeida, G. A. (1987), On the variability of desert aerosol radiative characteristics, *J. Geophys. Res.*, *92*(D3), 3017-3026.

Fountoukis, C., and A. Nenes (2007), ISORROPIA II: a computationally efficient thermodynamic equilibrium model for K+-Ca2+-Mg2+-Nh(4)(+)-Na+-SO42--NO3--Cl--H2O aerosols, *Atmospheric Chemistry and Physics*, *7*(17), 4639-4659.

Guenther, A., T. Karl, P. Harley, C. Wiedinmyer, P. I. Palmer, and C. Geron (2006), Estimates of global terrestrial isoprene emissions using MEGAN (Model of Emissions of Gases and Aerosols from Nature), *Atmospheric Chemistry and Physics*, *6*, 3181-3210.

Jaffe, D., I. McKendry, T. Anderson, and H. Price (2003), Six 'new' episodes of trans-Pacific transport of air pollutants, *Atmos. Environ.*, *37*(3), 391-404.

Karydis, V. A., S. L. Capps, A. G. Russell, and A. Nenes (2012), Adjoint sensitivity of global cloud droplet number to aerosol and dynamical parameters, *Atmos. Chem. Phys. Discuss.*, *12*(5), 12081-12117.

Karydis, V. A., P. Kumar, D. Barahona, I. N. Sokolik, and A. Nenes (2011), On the effect of dust particles on global cloud condensation nuclei and cloud droplet number, *J. Geophys. Res.-Atmos.*, *116*.

Kuhns, H., E. M. Knipping, and J. M. Vukovich (2005), Development of a United States-Mexico emissions inventory for the Big Bend Regional Aerosol and Visibility Observational (BRAVO) Study, *Journal of the Air & Waste Management Association*, *55*(5), 677-692.

Lance, S., A. Nenes, and T. A. Rissman (2004), Chemical and dynamical effects on cloud droplet number: Implications for estimates of the aerosol indirect effect, *J. Geophys. Res.*, *109*(D22), doi: 10.1029/2004JD004596.

Olivier, J. G. J., and J. J. M. Berdowski (2001), Global emissions sources and sinks, in *The Climate System*, edited by J. Berdowski, Guicherit, R. and B.J. Heij, pp. 33-78, A.A. Balkema Publishers/Swets & Zeitlinger Publishers, Lisse, The Netherlands.

Streets, D. G., et al. (2003), An inventory of gaseous and primary aerosol emissions in Asia in the year 2000, *J. Geophys. Res.-Atmos.*, *108*(D21).

van der Werf, G. R., J. T. Randerson, L. Giglio, G. J. Collatz, P. S. Kasibhatla, and A. F. Arellano, Jr. (2006), Interannual variability in global biomass burning emissions from 1997 to 2004, *Atmospheric Chemistry and Physics*, *6*, 3423-3441.

Wolff, G. T. (1984), On the nature of nitrate in coarse continental aerosols, *Atmospheric Environment*, *18*(5), 977-981.